DR ATSUSHI ANDO (Orcid ID : 0000-0003-1586-0356)

Article type : Paper

Received date: 28-May-2018

Revised version received date: 01-Oct-2018

Accepted date: 07-Nov-2018

Post-Eocene intensification of deep-water circulation in the central South Pacific:

Micropaleontological clues from dredged sites along the eastern Manihiki Plateau margin

Atsushi Ando[1,2] | Junichiro Kuroda[3] | Reinhard Werner[4] | Kaj Hoernle[4,5] | Brian T. Huber[1]

[1]Department of Paleobiology, National Museum of Natural History, Smithsonian Institution, Washington, DC, USA;

[2]BugWare, Inc., Tallahassee, FL, USA;

[3]Atmosphere and Ocean Research Institute, the University of Tokyo, Chiba, Japan;

[4]GEOMAR, Helmholtz Centre for Ocean Research Kiel, Kiel, Germany;

[5]Institut for Geosciences, Christian-Albrechts University of Kiel, Kiel, Germany

Correspondence: Dr. Atsushi Ando, BugWare, Inc., 1615 Village Square Blvd., Suite 8, Tallahassee, FL 32309, USA. Tel.: +1 850 668 3894; fax: +1 850 536 6257; Emails: AndoA@si.edu, atsushi.ando@bugware.com

Abstract

Reconstruction of early Cenozoic deep-water circulation is one of the keys to modelling Earth's greenhouse-to-icehouse surface evolution, but it has long been hampered by the paucity of information from the central South Pacific. To help overcome this knowledge gap, we present new micropalaeontological data from dredged carbonates (R/V *Sonne* Expedition SO193) at several eastern volcanic salients of the Manihiki Plateau. Interestingly, despite appreciable longitudinal separations among the dredged sites, ages indicated by the foraminiferal assemblages are consistently around the Middle Eocene [including mixed Turonian (Late Cretaceous)/Eocene at a single site], suggesting widespread post-Eocene cessation of the pelagic sedimentation. By integrating with independent seismic and chronostratigraphic data (Deep Sea Drilling Project Leg 33) for large-scale erosion of top-Eocene–Oligocene sedimentary units on the eastern Manihiki Plateau, our results can be viewed as novel physical evidence for the intensification of central South Pacific deep-water circulation since the Eocene/Oligocene climatic transition.

1 | INTRODUCTION

The central part of the South Pacific has long been a vast data-poor area in the study of deep-time Cenozoic palaeoceanography, for which two main reasons are apparent, natural and artificial. For the natural reason, the pelagic sedimentary records of this area are limited by very low rates of sediment accumulation. This is manifested by an extensive field of red clay and Fe–Mn nodules on the seafloor, including the "South Pacific bare zone" where sedimentary layers are minimally developed or non-existent (e.g., Rea et al., 2006; Glasby, 2007). Another (artificial) reason is that central South Pacific palaeoceanography has received little attention in the history of scientific deep-sea drilling. This is in stark contrast to the surrounding oceanic domains (Antarctic Ocean, Southern Ocean, West Pacific, central/eastern equatorial Pacific), which are characterized by superior sedimentary records and have been the foci of in-depth Cenozoic palaeoceanographic and palaeoclimatic studies. This mega-data bias is apparent from graphic compilations of palaeoceanographically studied deep-sea sites for stable isotopes [see, for example, Cramer et al., (2009, figure 1 therein)] and Nd isotopes (see later discussion).

Under such circumstances, one notable exception is the Manihiki Plateau (Figure 1), on which a continuous pelagic sedimentary record of the Cenozoic (Eocene and younger), perhaps of high palaeoceanographic potential, was proven to exist by Deep Sea Drilling Project (DSDP) Leg 33 (Shipboard Scientific Party, 1976). Previous studies at DSDP Site 317 and a nearby piston core presented Eocene to recent benthic foraminiferal faunal trends (Boltovskoy and Watanabe, 1994;

Hayward et al., 2010), Miocene planktonic foraminiferal biostratigraphy (Thunell, 1981) and benthic foraminiferal stable isotopes (Woodruff, 1985; Woodruff and Savin, 1989, 1991), and integrated Plio-Pleistocene magneto-, bio- and isotope-stratigraphy (Schönfeld, 1995; Beiersdorf et al., 1995). Meaningful early Cenozoic palaeoceanographic information, however, is still critically lacking from this region of the South Pacific.

This study aims to shed new light on early Cenozoic palaeoceanography in the central South Pacific by presenting new information from the Manihiki Plateau. The studied material includes recently recovered dredged carbonates along the eastern plateau margin. Based on the evidence from foraminiferal micropalaeontology of the dredged carbonates as well as its integration with past DSDP Leg 33 geological and geophysical data from the eastern plateau, a new reconstruction can be developed for a peculiar pattern of pelagic sedimentation over this setting. Results are placed in the context of established early Cenozoic events in global deep-water circulation, and are anticipated to direct more attention to this palaeoceanographically highly underexplored area.

2 | CRUISE INFORMATION

In 2007, IFM-GEOMAR Project SO193 was conducted using German R/V *Sonne*, sailing across the entire Manihiki Plateau and adjacent areas (Figure 1). The major goal of this expedition was to carry out systematic geological investigation on the plateau in terms of its origin, spatial–temporal

evolution and relationship with other mid-Cretaceous Pacific large igneous provinces (e.g., Timm et al., 2011; Golowin et al., 2017). In addition to bathymetric mapping and profiling, rock sampling by dredging was carried out on all major geomorphological features at a total of 82 sites (Figure S1). Technical methods of dredging as well as a first-order description of the dredged material can be found in Werner and Hauff (2007). Due to the strategy of targeting faults and scarps for igneous rock sampling, dredged samples were outnumbered by lavas and volcaniclastic rocks, yet some areas of the plateau were found to yield partially to strongly indurated sediments.

3 | MATERIAL AND METHODS

Among 37 dredged sites marked by the recovery of sedimentary rocks, several sites with blocks of light-coloured, apparently pelagic chalks/limestones with minor Fe–Mn precipitates were selected for foraminiferal analysis (Table S1). In addition to the main procedure of sample processing and analysis as detailed below, part of these samples as well as those from some other sites with carbonate-poor lithology were chosen for thin-section examination.

For foraminiferal analysis, each sample was cut into small (~0.5 cm-sided) pieces and weighed for 5 g (or less, depending on rock hardness), treated with 3% hydrogen peroxide (HP) solution, wet-sieved and dried. The <2 mm sieve fraction was saved for microscopic analysis. This conventional process is hereafter called the "1st HP" step, yet it resulted in only partial disaggregation for all

samples, leaving residue of variable foraminiferal abundance. The remaining very coarse (≥2 mm) fraction was then processed by the glacial acetic acid (GAC) method (e.g., Ando et al., 2008). Specifically, each of the remaining very coarse fractions was oven-dried, soaked in 100% CH_3COOH and then rinsed thoroughly with tap water (or stored in water for a few hours) until complete cessation of the chemical reaction. Disaggregation of this remaining harder fraction still did not proceed, but it was accidentally found that an additional round of drying and 3% HP treatment could facilitate the process with ease for some samples. This additional cycle of sample processing is hereafter called the "GAC/2nd HP" step.

Since this study focuses on age determination of dredged carbonates with varying sample processing results, foraminiferal picking and species identification were mostly limited to the >212 μm dry-sieve fraction, thus excluding small, often hardly identifiable specimens in the background assemblage. For prolific foraminiferal samples, specimen picking was performed qualitatively, using entire grid transect(s) of evenly spread foraminiferal residue on a picking tray until a sufficient number of specimens were collected. As described below, foraminiferal assemblages were completely different between the 1st HP and GAC/2nd HP steps. Foraminifera in the former are obviously from surficial, less stiff, younger sedimentary components, whereas those in the latter are considered to represent the essential sedimentary components at each site. It is noteworthy that specimens treated by GAC are found variably, often splendidly, preserved. The foraminiferal occurrences and counts are summarized in Table S2.

4 | RESULTS

Sites DR72 and DR69 yielded similar and the most intriguing foraminiferal assemblages (Figures 2 and 3). Recovered specimens are fairly well-preserved in terms of gross morphology, though more or less affected by recrystallization (Figure S2). At each site, the main assemblage components (extracted by GAC/2nd HP) are abundant, diverse Middle Eocene planktonic taxa, of which particularly age-diagnostic are species of *Acarinina*, *Globigerinatheka*, *Hantkenina* and *Morozovelloides* [identification of Eocene planktonic foraminifera in this study follows Pearson et al. (2006)]. The subordinate components (by 1st HP) are the Plio-Pleistocene taxa. Some taxa do not fall in these age intervals, indicating a certain extent of foraminiferal reworking from wider age ranges. This within-sample time-mixing is understandable considering the nature of the unstable depositional setting at narrow, steep, current-susceptible volcanic salient tops.

Site DR93, likewise, yields a Middle Eocene planktonic assemblage (by GAC/2nd HP) including species of *Acarinina*, *Globigerinatheka*, *Morozovelloides* and *Turborotalia* (Figure 4). Minor time-mixing within the Eocene is also likely in this sample. No subordinate Neogene taxa are present. Thin-section examination indicates that Eocene planktonic foraminifera are prolific in this sample, with even higher diversity than that observed in the washed sample (Figure S3a).

Site DR82 is marked by rare isolated specimens (by both 1st and 2nd steps) (Figure 5), contrasting with the sites described above. Based on thin section analyses, however, actual foraminiferal abundance and diversity can be rated as very high (Figures 5 and S3b–S3d). Several species of *Acarinina* and *Morozovella* (with characteristic muricate surface/keel), most likely representing an assemblage from the Middle Eocene, are identified. Moreover, this sample is exceptional in containing a few taxa of Turonian (Late Cretaceous) planktonic foraminifera that are very poorly preserved but are still identifiable at the species level. Taphonomically of interest are numerous fragmented specimens comprising chamber-fillings of clinoptilolite, occasionally occurring as complete internal moulds (Figure 5f,j,k; see also Figure 4f).

Other Sites DR 67, DR 68 and DR97 (of which the last is located off the southwestern plateau) are marked by Neogene planktonic foraminifera only (after 1st HP). At each site, the assemblage is accompanied by some extinct Neogene taxa (Figure 6), suggesting very slow rates of sediment accumulation and within-Neogene time-mixing.

5 | SIGNIFICANCE OF UBIQUITOUS EOCENE SURFACE SEDIMENTS

The observed congruence in the ages of the dredged carbonates at the Middle Eocene is unexpected and intriguing, especially because the studied sites are the sedimentary caps on several volcanic salients that are widely separated from each other along the eastern Manihiki Plateau margin

(Figures 1 and 7). The number of examined sites is rather few, but it is sufficient to suggest a certain genetic background mechanism.

The ubiquity of Middle Eocene surface sediments can be attributed to primary palaeoceanographic factor(s) that controlled pelagic sedimentation over this oceanic domain. Note that secondary gravitational processes (slumping) of younger (Oligocene–Neogene) sediments is unlikely to explain the widespread exposure of an Eocene lithologic unit, as this would necessitate multiple coincidences of local processes. There are three possible options, since the Eocene there has been: (1) a substantial decrease in primary calcium carbonate production; (2) prevalence of carbonate dissolution on the seafloor; and/or (3) a change in deep-water physical properties that created unfavourable conditions for the settling of pelagic sedimentary particles. The former two possibilities can be ruled out because nearby DSDP Site 317 provides evidence for continuous Cenozoic pelagic sedimentation in this area (Figure 7), and because the dredged depths (Table S1) are well above Cenozoic carbonate compensation depths (CCDs) (Pälike et al., 2012).

Thus, the most plausible explanation for the inferred widespread cessation of pelagic sedimentation is a change in deep-water physical properties. Specifically, the preferred mechanism is a post-Eocene shift in or intensification of deep-water circulation in terms of flow velocity (increased current velocity exceeding a threshold of sediment settling), flow thickness (increased height of the water circulation cell), flow direction (development of an easterly/southerly deep-water current directly bathing the eastern Manihiki Plateau), or a combination of these.

Strong support for this interpretation comes from DSDP Leg 33 data (Schlanger and Winterer, 1976; Shipboard Scientific Party, 1976; Takayanagi and Oda, 1976). Based on integration of Site 317 chronostratigraphic results with seismic profiles (Figure S4), widespread seafloor erosion and exposure of the top-Eocene–Oligocene lithologic units are obvious in the eastern low-gradient flank of the Manihiki Plateau (Figures 7 and S5). Considering that its water depth was shallower than the Pacific CCD during the Oligocene–Neogene (4–4.5 km: Pälike et al., 2012), the only mechanism for explaining the significant erosion of post-Eocene sediments on the plateau is intensification of abyssal currents that have prevented sediment settling since that time. It should be noted that the summit of the Manihiki Plateau is still covered with coherent Neogene chalk/ooze layers (Figures 7 and S5), showing no evidence for widespread current-induced erosion, despite having sufficient depth to have been influenced by such an abyssal current. This fact does not necessarily contradict our interpretation by invoking the development of an inherent current system surrounding a seamount. That is, the plateau summit could have been topped by a water cell of downward circulation (thus facilitating retention of sediment particles), whereas, at the same time, the flank setting of the upper plateau could have been swept by horizontal circular currents (e.g., Arreguín-Rodríguez et al., 2016).

6 | BROADER PALAEOCEANOGRAPHIC IMPLICATION

Based on the observed timing for the onset of non-deposition on the eastern Manihiki Plateau, it would be natural to correlate the inferred major shift in South Pacific deep-water circulation with the Eocene–Oligocene climatic transition. It is one of the best known and studied palaeoenvironmental events in Earth's history in relation to the onset of the Antarctic Circumpolar Current (Figure 8), the development of North Atlantic Deep Water, the expansion of Antarctic ice sheets, and the lowering of CO_2 (e.g., Katz et al., 2011; Goldner et al., 2014; Scher et al., 2015; Coxall et al., 2018).

In conjunction with the Eocene/Oligocene climatic transition, there is a series of physical evidence for deep-water circulation shifts in and around the South Pacific, correlating well with the results of this study. They are: bottom current-controlled erosion and redeposition in the Samoan Passage (Johnson, 1974; Hollister et al., 1974) (Figures 1 and 8b); widespread deep-sea unconformities revealed by multiple DSDP Leg 21 sites in the western South Pacific off Australia (Kennett et al., 1972, 1975) (Figure 8b), and radiolarian reworking events in the central equatorial Pacific (Moore, 2013). A coeval widespread hiatus is also known from the Southern Ocean (Wright and Miller, 1993; Cramer et al., 2009). In addition, Boltovskoy and Watanabe (1994) documented a major Eocene/Oligocene boundary faunal turnover of benthic foraminifera at Site 317.

As noted above (Section 1), the central South Pacific is a markedly data-poor area for Cenozoic palaeoceanography. Although recent progress in seawater Nd isotopic studies (mainly from fish debris and Fe–Mn crusts) has been generating crucial insights into past deep-water circulation patterns, data from the central South Pacific are limited to a couple of case studies with coarse age resolution (van de Flierdt et al., 2004; Thomas et al., 2014) (Figure 8). Of these, van de Flierdt et al. (2004) analysed a 38-Myr-spanning Fe–Mn crust (called "Nova") from the Samoan Passage (Figures 1 and 8b) and interpreted the Nd isotopic time-series as reflecting late Eocene(?) onset of the Deep Western Boundary Current. Nonetheless, while Nd isotopes are excellent tracers of sources of deep-water masses, they provide limited clues to the flow intensity of water circulation, as pointed out previously (e.g., Lyle et al., 2007). Therefore, our new view on the post-Eocene flow intensification of South Pacific deep water, as deciphered from physical evidence of non-deposition/erosion of the eastern Manihiki Plateau and its salients, will be invaluable in filling this major palaeoceanographic knowledge gap.

ACKNOWLEDGEMENTS

The R/V *Sonne* Expedition SO193 (Manihiki) was funded by the German Ministry of Education and Research (BMBF, Grant 03G0193A to K.H.). The lead author thanks Hiroki Hayashi (Shimane University, Japan) for his help with identification of Plio-Pleistocene planktonic foraminifera, and

Koichi Momma (National Museum of Nature and Science, Japan) for visual identification of diagenetic phases of minerals. Scanning electron microscopic (SEM) study of foraminifera was performed at the SEM Lab of the National Museum of Natural History, Smithsonian Institution; some of the specimen SEM images were taken by Jo Ann Sanner.

REFERENCES

Ando, A., Kaiho, K., Kawahata, H. and Kakegawa, T., 2008. Timing and magnitude of early Aptian extreme warming: Unraveling primary $\delta^{18}O$ variation in indurated pelagic carbonates at Deep Sea Drilling Project Site 463, central Pacific Ocean. *Palaeogeogr., Palaeoclimatol., Palaeoecol.*, **260**, 463–476.

Arreguín-Rodríguez, G.J., Alegret, L. and Thomas, E., 2016. Late Paleocene-middle Eocene benthic foraminifera on a Pacific seamount (Allison Guyot, ODP Site 865): Greenhouse climate and superimposed hyperthermal events. *Paleoceanography*, **31**, doi:10.1002/2015PA002837.

Aze, T., Ezard, T.H.G., Purvis, A., Coxall, H.K., Stewart, D.R.M., Wade, B.S. and Pearson, P.N., 2011. A phylogeny of Cenozoic macroperforate planktonic foraminifera from fossil data. *Biol. Rev.*, **86**, 900–927.

Beiersdorf, H. Bickert, T. Cepek, P., Fenner, J., Petersen, N., Schönfeld, J., Weiss, W. and Won, M.-Z., 1995. High-resolution stratigraphy and the response of biota to Late Cenozoic environmental changes in the central equatorial Pacific Ocean (Manihiki Plateau). *Mar. Geol.*, **125**, 29–59.

Boltovskoy, E. and Watanabe, S., 1994. Biostratigraphy of Tertiary and Quaternary benthic bathyal foraminifers of DSDP Site 317 (Tropical Pacific). *Mar. Micropaleontol.*, **23**, 101–120.

Coxall, H.K., Huck, C.E., Huber, M., Lear, C.H., Legarda-Lisarri, A., O'Regan, M., Sliwinska, K.K., van de Flierdt, T., de Boer, A.M., Zachos, J.C. and Backman, J., 2018. Export of nutrient rich Northern Component Water preceded early Oligocene Antarctic glaciation. *Nat. Geosci.*, **11**, 190-196.

Cramer, B.S., Toggweiler, J.R., Wright, J.D., Katz, M.E. and Miller, K.G., 2009. Ocean overturning since the Late Cretaceous: Inferences from a new benthic foraminiferal isotope compilation. *Paleoceanography*, **24**, PA4216, doi:10.1029/2008PA001683.

Glasby, G.F., 2007. Broad region of no sediment in the southwest Pacific Basin: COMMENT AND REPLY: COMMENT. *Geology*, **35**, e132.

Goldner, A., Herold, N. and Huber, M., 2014. Antarctic glaciation caused ocean circulation changes at the Eocene–Oligocene transition. *Nature*, **511**, 574–577.

Golowin, R., Portnyagin, M., Hoernle, K., Hauff, F., Gurenko, A., Garbe-Schönberg, D., Werner, R. and Turner, S., 2017. Boninite-like intraplate magmas from Manihiki Plateau require ultra-depleted and enriched source components. *Nat. Commun.,* **8**, 14322, doi:10.1038/ncomms14322.

Hague, A.M., Thomas, D.J., Huber, M., Korty, R., Woodard, S.C. and Jones, L.B., 2012. Convection of North Pacific deep water during the early Cenozoic. *Geology*, **40**, 527–530.

Hall, I.R., McCave, I.N., Zahn, R., Carter, L., Knutz, P.C. and Weedon, G.P., 2003. Paleocurrent reconstruction of the deep Pacific inflow during the middle Miocene: Reflections of East Antarctic Ice Sheet growth. *Paleoceanography*, **18**, 1040, doi:10.1029/2002PA000817.

Hayward, B.W., Johnson, K., Sabaa, A.T., Kawagata, S. and Thomas, E., 2010. Cenozoic record of elongate, cylindrical, deep-sea benthic foraminifera in the North Atlantic and equatorial Pacific Oceans. *Mar. Micropaleontol.*, **74**, 75–95.

Hollister, C.D., Johnson, D.A. and Lonsdale, P.F., 1974. Current-controlled abyssal sedimentation: Samoan Passage, equatorial West Pacific. *J. Geol.*, **82**, 275–300.

Huck, C.E., van de Flierdt, T., Bohaty, S.M. and Hammond, S.J., 2017. Antarctic climate, Southern Ocean circulation patterns, and deep water formation during the Eocene. *Paleoceanography*, **32**, 674–691.

Johnson, D.A., 1974. Deep Pacific circulation: intensification during the Early Cenozoic. *Mar. Geol.*, **17**, 71–78.

Katz, M.E., Cramer, B.S., Toggweiler, J.R., Esmay, G., Liu, C., Miller, K.G., Rosenthal, Y., Wade, B.S. and Wright, J.D., 2011. Impact of Antarctic Circumpolar Current development on late Paleogene ocean structure. *Science*, **332**, 1076–1079.

Kennett, J.P., Burns, R.E., Andrews, J.E., Churkin Jr., M., Davies, T.A., Dumitrica, P., Edwards, A.R., Galehouse, J.S., Packham, G.H. and van der Lingen, G.J., 1972. Australian–Antarctic continental drift, palaeocirculation changes and Oligocene deep-sea erosion. *Nat. Phys. Sci.*, **239**, 51–55.

Kennett, J.P., Houtz, R.E., Andrews, P.B., Edwards, A.R., Gostin, V.A., Hajós, M., Hampton, M.A., Jenkins, D.G., Margolis, S.V., Ovenshine, A. T. and Perch-Nielsen, K., 1975. Cenozoic paleoceanography in the southwest Pacific Ocean, Antarctic glaciation, and the development of the Circum-Antarctic Current. In: *Initial Reports of the Deep Sea Drilling Project*, *vol. 29* (J.P. Kennett, R.E. Houtz, et al.) U.S. Government Printing Office, Washington, D.C., 1155–1169.

Le Houedec, S., Meynadier, L., Cogné, J.-P., Allègre, C.J. and Gourlan, A.T., 2012. Oceanwide imprint of large tectonic and oceanic events on seawater Nd isotope composition in the Indian Ocean from 90 to 40 Ma. *Geochem. Geophys. Geosyst.*, **13**, Q06008, doi:10.1029/2011GC003963.

Le Houedec, S., Meynadier, L. and Allègre, C.J., 2016. Seawater Nd isotope variation in the Western Pacific Ocean since 80 Ma (ODP 807, Ontong Java Plateau). *Mar. Geol.*, **380**, 138–147.

Lyle, M., Gibbs, S., Moore, T.C. and Rea, D.K., 2007. Late Oligocene initiation of the Antarctic Circumpolar Current: Evidence from the South Pacific. *Geology*, **35**, 691–694.

Martin, E.E. and Scher, H., 2006. A Nd isotopic study of southern sourced waters and Indonesian Throughflow at intermediate depths in the Cenozoic Indian Ocean. *Geochem. Geophys. Geosyst.*, **7**, Q09N02, doi:10.1029/2006GC001302.

Moore Jr., T.C., 2013. Erosion and reworking of Pacific sediments near the Eocene-Oligocene boundary. *Paleoceanography*, **28**, doi:10.1002/palo.20027.

Pälike, H., Lyle, M.W., Nishi, H., Raffi, I., Ridgwell, A., Gamage, K., Klaus, A., Acton, G., Anderson, L., Backman, J., Baldauf, J., Beltran, C., Bohaty, S.M., Bown, P., Busch, W., Channell, J.E.T., Chun, C.O.J., Delaney, M., Dewangan, P., Dunkley Jones T.,, Edgar, K.M., Evans, H., Fitch, P., Foster, G.L., Gussone, N., Hasegawa, H., Hathorne, E.C., Hayashi, H., Herrle, J.O., Holbourn, A., Hovan, S., Hyeong, K., Iijima, K., Ito, T., Kamikuri, S., Kimoto, K., Kuroda, J., Leon-Rodriguez, L., Malinverno, A., Moore Jr., T.C., Murphy, B.H., Murphy, D.P., Nakamura, H., Ogane, K., Ohneiser, C., Richter, C., Robinson, R., Rohling, E.J., Romero, O., Sawada, K., Scher, H., Schneider, L., Sluijs, A., Takata, H., Tian, J., Tsujimoto, A., Wade, B.S., Westerhold, T., Wilkens, R., Williams, T., Wilson, P.A., Yamamoto, Y., Yamamoto, S., Yamazaki, T. and Zeebe, R.E., 2012. A Cenozoic record of the equatorial Pacific carbonate compensation depth. *Nature*, **488**, 609–614.

Pearson, P.N., Olsson, R.K., Huber, B.T., Hemleben, C. and Berggren, W.A. (eds.), 2006. *Atlas of Eocene Planktonic Foraminifera*. *Cushman Found. Spec. Publ.*, **41**.

Rea, D.K., Lyle, M.W., Liberty, L.M. Hovan, S.A., Bolyn, M.P., Gleason, J.D., Hendy, I.L., Latimer, J.C., Murphy, B.M., Owen, R.M., Paul, C.F., Rea, T.H.C., Stancin, A.M., Thomas, D.J., 2006. Broad region of no sediment in the southwest Pacific Basin. *Geology*, **34**, 873–876.

Sallée, J.-B., Speer, K., Rintoul, S. and Wijffels, S., 2010. Southern Ocean thermocline ventilation. *J. Phys. Oceanogr.*, **40**, 509–529.

Scher, H.D., Bohaty, S.M., Zachos, J.C. and Delaney, M.L., 2011. Two-stepping into the icehouse: East Antarctic weathering during progressive ice-sheet expansion at the Eocene–Oligocene transition. *Geology*, **39**, 383–386.

Scher, H.D., Whittaker, J.M., Williams, S.E., Latimer, J.C., Kordesch, W.E.C. and Delaney, M.L., 2015. Onset of Antarctic Circumpolar Current 30 million years ago as Tasmanian Gateway aligned with westerlies. *Nature*, **523**, 580–583.

Schlanger, S.O. and Winterer, E.L., 1976. Underway geophysical data: Navigation, bathymetry, magnetics, and seismic profiles. In: *Initial Reports of the Deep Sea Drilling Project*, *vol. 33* (S.O. Schlanger, E.D. Jackson, et al.) U.S. Government Printing Office, Washington, D.C., 655–693.

Schönfeld, J., 1995. Biostratigraphy and assemblage composition of benthic foraminifera from the Manihiki Plateau, southwestern tropical Pacific. *J. Micropalaeontol.*, **14**, 165–175.

Shipboard Scientific Party, 1976. Site 317. In: *Initial Reports of the Deep Sea Drilling Project*, *vol. 33* (S.O. Schlanger, E.D. Jackson, et al.) U.S. Government Printing Office, Washington, D.C., 161–300.

Takayanagi, Y. and Oda, M., 1976. Shore laboratory report on Cenozoic planktonic foraminifera: Leg 33. In: *Initial Reports of the Deep Sea Drilling Project*, *vol. 33* (S.O. Schlanger, E.D. Jackson, et al.) U.S. Government Printing Office, Washington, D.C., 451–465.

Thomas, D.J., 2004. Evidence for deep-water production in the North Pacific Ocean during the early Cenozoic warm interval. *Nature*, **430**, 65-68.

Thomas, D.J., Lyle, M., Moore Jr., T.C. and Rea, D.K., 2008. Paleogene deepwater mass composition of the tropical Pacific and implications for thermohaline circulation in a greenhouse world. *Geochem. Geophys. Geosyst.*, **9**, Q02002, doi:10.1029/2007GC001748.

Thomas, D.J., Korty, R., Huber, M., Schubert, J.A. and Haines, B., 2014. Nd isotopic structure of the Pacific Ocean 70–30 Ma and numerical evidence for vigorous ocean circulation and ocean heat transport in a greenhouse world. *Paleoceanography*, **29**, 454–469.

Thunell, R.C., 1981. Late Miocene–early Pliocene planktonic foraminiferal biostratigraphy and paleoceanography of low-latitude marine sequences. *Mar. Micropaleontol.*, **6**, 71–90.

Timm, C., Hoernle, K., Werner, R., Hauff, F., van den Bogaard, P., Michael, P., Coffin, M.F. and Koppers, A., 2011. Age and geochemistry of the oceanic Manihiki Plateau, SW Pacific: New evidence for a plume origin. *Earth Planet. Sci. Lett.*, **304**, 135–146.

van de Flierdt, T., Frank, M., Halliday, A.N., Hein, J.R., Hattendorf, B., Günther, D. and Kubik, P.W., 2004. Deep and bottom water export from the Southern Ocean to the Pacific over the past 38 million years. *Paleoceanography*, **19**, PA1020, doi:10.1029/2003PA000923.

Wade, B.S., Pearson, P.N., Berggren, W.A. and Pälike, H., 2011. Review and revision of Cenozoic tropical planktonic foraminiferal biostratigraphy and calibration to the geomagnetic polarity and astronomical time scale. *Earth-Sci. Rev.*, **104**, 111–142.

Weaver, A.J., Bitz, C.M., Fanning, A.F. and Holland, M.M., 1999. Thermohaline circulation: High-latitude phenomena and the difference between the Pacific and Atlantic. *Annu. Rev. Earth Planet. Sci.*, **27**, 231–285.

Werner, R. and Hauff, F. (eds.), 2007. *FS Sonne, Fahrtbericht / Cruise Report SO193 MANIHIKI: Temporal, Spatial, and Tectonic Evolution of Oceanic Plateaus, Suva/Fiji – Apia/Samoa, 19.05. - 30.06.2007.* IFM-GEOMAR Report 13, IFM-GEOMAR, Kiel, 201 pp., doi:10.3289/ifm-geomar_rep_13_2007.

Woodruff, F., 1985. Changes in Miocene deep-sea benthic foraminiferal distribution in the Pacific Ocean: Relationship to paleoceanography. In: *The Miocene Ocean: Paleoceanography and Biogeography* (J.P. Kennett, ed.) *Geol. Soc. Am. Mem.*, **163**, 131–176.

Woodruff, F. and Savin, S.M., 1989. Miocene deepwater oceanography. *Paleoceanography*, **4**, 87–140.

Woodruff, F. and Savin, S.M., 1991. Mid-Miocene isotope stratigraphy in the deep sea: High resolution correlations, paleoclimatic cycles, and sediment preservation. *Paleoceanography*, **6**, 755–806.

Wright, J.D. and Miller, K.G., 1993. Southern Ocean influences on late Eocene to Miocene deepwater circulation. In: *The Antarctic Paleoenvironment: A Perspective on Global Change* (J.P. Kennett and D.A. Warnke, eds.) *Antarct. Res. Ser.*, **60**, 1–25.

Wright, N.M., Scher, H.D., Seton, M., Huck, C.E. and Duggan, B.D., 2018. No change in Southern Ocean circulation in the Indian Ocean from the Eocene through late Oligocene. *Paleoceanogr. Paleoclimatol.*, **33**, 152–167.

Figure and Appendix captions

FIGURE 1 (a) Bathymetric map of the Manihiki Plateau, South Pacific, showing site locations of dredged sedimentary rocks by R/V *Sonne* Expedition SO193 analysed in this study (red circles with prefix "DR") (Werner and Hauff, 2007). Also shown are locations of DSDP Site 317 (Shipboard Scientific Party, 1976), Samoan Passage piston cores (80, 82, 88) by Johnson (1974), and Fe–Mn crust "Nova" (D137-01) by van de Flierdt et al. (2004). Lines A–E–H and J–N (corresponding to those in Figures 7 and S5) indicate parts of DSDP Leg 62 ship tracks, from which seismic profiles adopted in this study were released by Schlanger and Winterer (1976). This colour bathymetric map was generated using The Generic Mapping Tools, version 5.2.1 (c) 1991–2015 (P. Wessel, W.H.F. Smith, R. Scharroo, J. Luis and F. Wobbe) and database The GEBCO_2014 Grid, version 20150318, http://www.gebco.net. (b) Present-day global map showing tectonic plate configuration and position of the Manihiki Plateau (MP) [enclosed by red line delineating area of (a)], as well as major paths of deep-water circulation (Weaver et al., 1999; Hall et al., 2003; Sallée et al., 2010). AAC—Antarctic Circumpolar Current; DWBC—Deep Western Boundary Current. (c) Middle Eocene palaeo-position of the Manihiki Plateau on 45 Ma palaeogeographic and plate tectonic reconstruction. For (b) and (c), base maps (orthographic projections) were generated using ODSN Plate Tectonic Reconstruction Service (http://www.odsn.de/odsn/services/paleomap/paleomap.html).

FIGURE 2 SEM images of Eocene planktonic foraminifera from Sample DR72-2 (a–r) and Sample DR69-1 (s). All scale bars = 100 µm. Asterisks (*) indicate specimens isolated by glacial acetic acid treatment. (a) *Hantkenina lehneri*, with numerous phillipsite crystals attached. (b) *Hantkenina dumblei*. (c) *Hantkenina liebusi*. (d) *Morozovelloides lehneri*. (e) *Morozovella crater*. (f) *Morozovelloides bandyi*. (g) *Morozovelloides* aff. *M. coronatus*. (h,i) *Globigerinatheka curryi.* (j) *Globigerinatheka kugleri*. (k) *Acarinina praetopilensis*. (l) *Acarinina pseudosubsphaerica*. (m) *Acarinina rohri*. (n) *Subbotina senni*. (o) *Subbotina gortanii*. (p) *Subbotina corpulenta*. (q) *Subbotina roesnaesensis*. (r) *Praemurica? lozanoi*. (s) *Globigerinatheka barri*.

FIGURE 3 Diagram showing within-sample age variation of dredged carbonates at Sites DR69 and DR72. Numerical age ranges of planktonic foraminifera are from Aze et al. (2011), and timescale is from Aze et al. (2011) and Wade et al. (2011). Thick-lined ranges are major taxa occurring in few/common to abundant proportions (>4% of total assemblage at either 1st or 2nd sample processing step). Grey horizontal bars represent most essential ages of surface sediments at these sites. Also shown at further right is the possible age range of Sample DR82-4 (from base of *A. praetopilensis* to top of *Mz. aragonensis*). Plio.—Pliocene; Pleisto.—Pleistocene; E—Early; M—Middle; L—Late.

FIGURE 4 (Left) SEM and thin-section images of Eocene planktonic foraminifera from Samples DR93-9 (a–e,g,h) and DR93-6 (f). Scale bars = 100 µm unless indicated otherwise. Asterisks (*) indicate specimens isolated by glacial acetic acid treatment. (a) *Turborotalia cerroazulensis*. (b) *Turborotalia pomeroli*. (c) *Morozovelloides crassatus*. (d) *Acarinina bullbrooki*. (e) *Catapsydrax globiformis*. (f) *Globigerinatheka semiinvoluta?*, whole specimen (1) and surface ultrastructure (2) of complete clinoptilolite internal mould. (g) *Acarinina topilensis*. (h) *Morozovelloides bandyi*. (Right) Diagram showing within-sample age variation at this site (see Figure 3 for information).

FIGURE 5 Various microscopic images of planktonic foraminifera from Samples DR82-4 (a,f–m) and DR82-5 (b–e) [Eocene (a–g) and Turonian (h–m)]. Scale bars = 100 µm unless indicated otherwise. Asterisks (*) indicate specimens isolated by glacial acetic acid treatment. (a) *Morozovella aragonensis*. (b) *Morozovella* sp. (*aragonensis* or *crater*). (c) *Acarinina* sp. (*cuneicamerata*?). (d) *Acarinina praetopilensis*. (e) *Subbotina* sp. (f) *Subbotina* sp. (*linaperta*?), whole specimen (1) and surface ultrastructure (2) of complete clinoptilolite internal mould. (g) *Parasubbotina* cf. *P. pseudowilsoni*. (h) *Dicarinella imbricata*. (i–k) *Marginotruncana pseudolinneiana*, with magnified chamber filling (j5) and complete internal mould (k) composed of clinoptilolite. (l) ?*Helvetoglobotruncana helvetica*. (m) *Marginotruncana* sp.

FIGURE 6 SEM and stereomicroscopic images of extinct Neogene planktonic foraminifera from Samples DR67-5 (a–c), DR68-3 (d) and DR97 (e–g). All scale bars = 100 µm. (a) *Dentoglobigerina venezuelana*. (b) *Globigerinoides primordius*. (c) *Dentoglobigerina larmeui*? (d) *Globigerinoides subquadratus*. (e) *Dentoglobigerina altispira*. (f) *Globigerinella obesa*. (g) *Catapsydrax dissimilis*.

FIGURE 7 Evidence for large-scale erosion of the top-Eocene–Oligocene lithologic unit, eastern Manihiki Plateau (MP), as seen in a sub-seafloor structural diagram based on seismic profiles along the DSDP Leg 33 ship track (Schlanger and Winterer, 1976) and DSDP Site 317 chronostratigraphy (Shipboard Scientific Party, 1976; Takayanagi and Oda, 1976). See Figure 1a for seismic track lines (A–E–H and J–N) and also Figures S4 and S5 for further information on the compilation of this diagram. mbsl—metres below sea level; sec.—two-way travel time (in seconds).

FIGURE 8 (a) Schematic of Middle–Late Eocene deep-water circulation in and around the Pacific Ocean, illustrated on a 45 Ma plate tectonic reconstruction. Labelled grey dots indicate DSDP/ODP/IODP sites (and single location of Fe–Mn crust) previously analysed for Nd-isotopic deep-water palaeoceanography at time-window of 48–34 Ma (Thomas, 2004; van de Flierdt et al., 2004; Martin and Scher, 2006; Thomas et al., 2008, 2014; Scher et al., 2011, 2015; Hague et al., 2012; Le Houedec et al., 2012, 2016; Huck et al., 2017; Wright et al., 2018). Arrows indicate flow path

reconstructions based on Hague et al. (2012), Thomas et al. (2014), Le Houedec et al. (2016) and Huck et al. (2017). Broken arrows and broken line express formation and northern limit of Southern Ocean-sourced deep water (e.g., Hague et al., 2012; Thomas et al., 2014), though its specific major path has not been illustrated by any of the previous studies. (b) Schematic mid-Oligocene deep-water circulation on a 30 Ma plate tectonic reconstruction. Grey dots are previous deep-sea sites analysed for Nd isotopes (as above) at 34–28.5 Ma [citations same as in (a) except for Thomas (2004)], and grey triangles are DSDP sites of widespread Oligocene unconformities at Lord Howe Rise and Coral Sea (Kennett et al., 1972, 1975). Flow path interpretations are based on Kennett et al. (1975), van de Flierdt et al. (2004), Hague et al. (2012) and Wright et al. (2017); proto-Deep Western Boundary Current (see also Figure 1b) is depicted to account for Samoan Passage (SP) erosion (Johnson, 1974; Hollister et al., 1974). Bifurcate arrow toward the Manihiki Plateau is to visualize proposed post-Eocene flow intensification of central South Pacific deep water by this study. For (a) and (b), base maps (equidimensional cylindrical projections) were generated using ODSN Plate Tectonic Reconstruction Service (http://www.odsn.de/odsn/services/paleomap/paleomap.html).

Table S1 Summary of site information on dredging “on/off bottom” location and water depth by R/V *Sonne* Expedition SO193, and lithology of dredged sedimentary rocks examined.

Table S2 Foraminiferal count data from DR sample series of R/V *Sonne* Expedition SO193 (Eocene planktonic taxa highlighted).

FIGURE S1 Detailed sampling map of R/V *Sonne* Expedition SO193 across the Manihiki Plateau. Adopted from Werner and Hauff (2007, appendix V therein).

FIGURE S2 Selected SEM images of Eocene planktonic foraminifera from Sample DR72-2, showing preservation states in magnified surface views. (a) *Morozovella crater* (= Figure 2e in main text). Example of best-preserved specimen with pored wall surface that appears nearly intact, but with muricae/pustules that are thoroughly accentuated by blocky recrystallized calcite. (b) *Subbotina senni* (= Figure 2n). Another seemingly very well-preserved specimen, yet wall surface is evenly augmented by micron-scale secondary calcite crystals. (c) *Globigerinatheka curryi* (= Figure 2h). Specimen in more advanced stage of recrystallization.

FIGURE S3 Thin-section photomicrograph pairs [open (upper) and cross-polarized (lower) for each] of selected samples. (a) Samples DR93-6 and (b) DR82-5. Note very abundant planktonic foraminifera that are most likely Eocene in age. (c,d) Sample DR82-4, showing common presence of Late Cretaceous planktonic foraminifera (*Marginotruncana pseudolinneiana* group). Note rectangular and double-keeled cross-sections characteristic of this species.

FIGURE S4 Correlation between chronostratigraphic and seismic data, DSDP Site 317, eastern Manihiki Plateau. Combined black-and-white image (right) is original Leg 33 litho-, bio- and seismic-stratigraphy adopted from Schlanger and Winterer (1976, figure 4 therein). In this study, Cenozoic (Middle Eocene and younger) age framework is revised using planktonic foraminiferal datums selected from Takayanagi and Oda (1976) [their studied levels shown aside datum listing (grey ticks)], calibrated against recent standard biochronology (Wade et al., 2011). Cretaceous to Early Eocene age assignments are from Shipboard Scientific Party (1976). For seismic unit column, colouring corresponds to that of Figures 7 and S5.

Planktonic foraminiferal range chart of selected taxa by Takayanagi and Oda (1976) is reproduced (left) for the interval 200–400 m below seafloor. It demonstrates that the Eocene/Oligocene transition could have been obscured, possibly due to the mechanism of deep-water circulation shift discussed in the main text. In this regard, noteworthy are the stratigraphic relationships of the base

of *Turborotalia ampliapertura* (orange circle) with the tops of *Catapsydrax africanus*, *Catapsydrax globiformis* and *Globigerinatheka index* (green circles). In the ideal Upper Eocene section, there exists a range overlap between *T. ampliapertura* and the latter three species (Pearson et al., 2006). Lack of such co-existence points to the presence of a sedimentation gap at Site 317B Eocene/Oligocene transition.

FIGURE S5 Compilation of DSDP Leg 33 seismic data for construction of sub-seafloor structural diagram in Figure 7. (a) Mosaic of seismic profiles (upper panel) using images of Schlanger and Winterer (1976, figure 2 therein), and its coloured sub-seafloor lithologic interpretation (lower panel) based on expansion of Site 317 chronostratigraphic data (Figure S4) along seismic reflectors. (b) Latitude–longitude coordinates of Leg 33 ship tracks from Schlanger and Winterer (1976, figure 1 therein), upon which a coloured sub-seafloor geologic profile is fitted as in Figure 7. Upper-case letters (A–N) are primary (bold) and secondary tie-points between seismic/colour geological profiles and Leg 33 ship track. “sec.”—two-way travel time (in seconds).

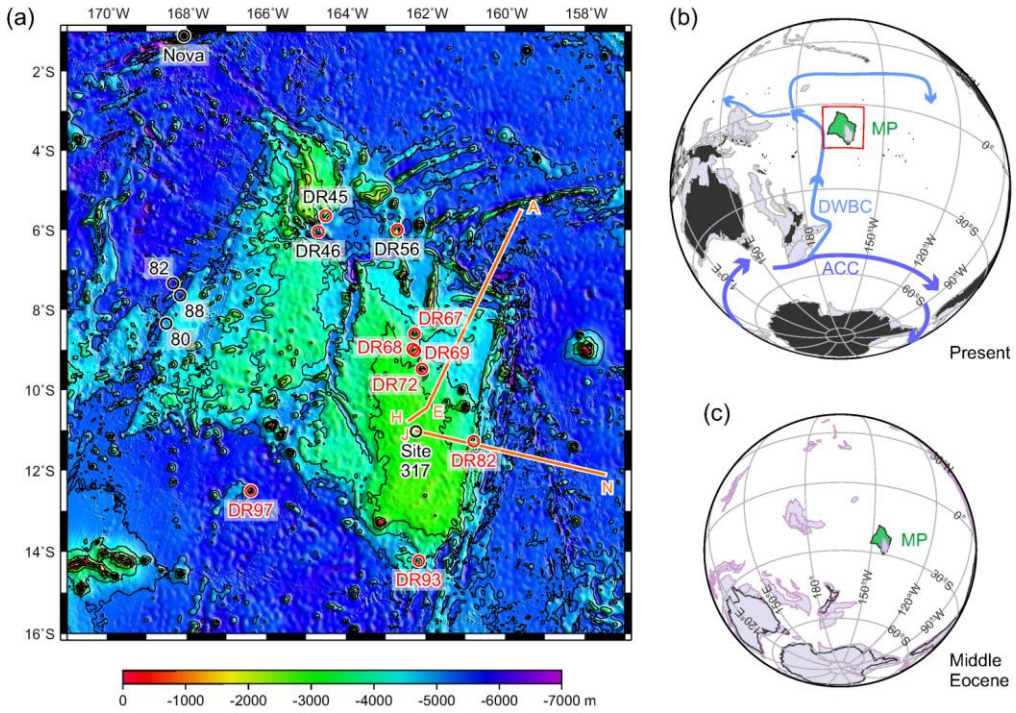

Ando et al. (2018MS)

Figure 1

100 % (179.9 × 125.1 mm)

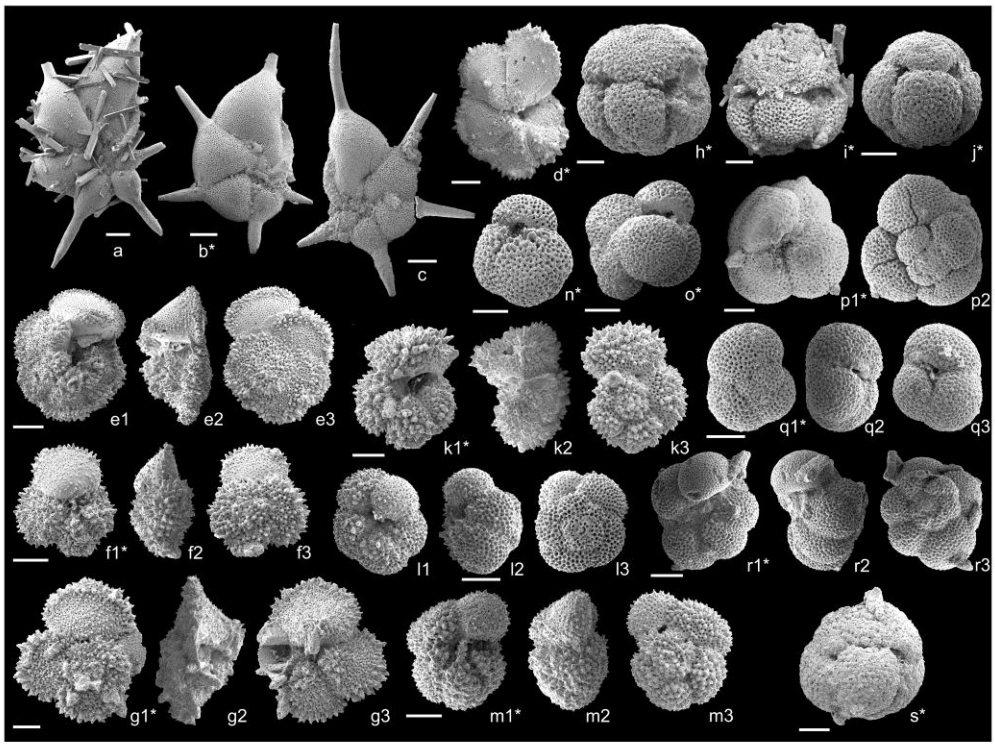

Ando et al. (2018MS)

Figure 2

100 % (177.0 × 132.0 mm)

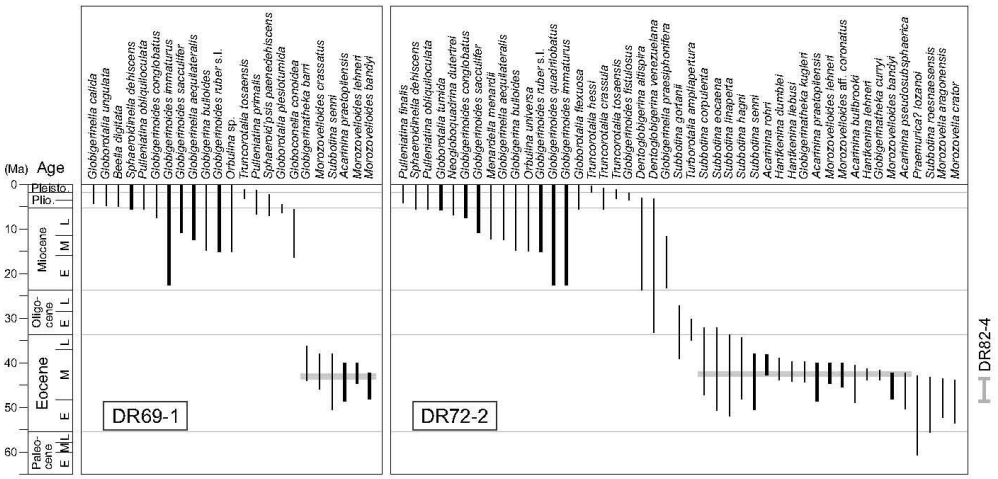

Ando et al. (2018MS)

Figure 3

100 % (176.8 × 84.0 mm)

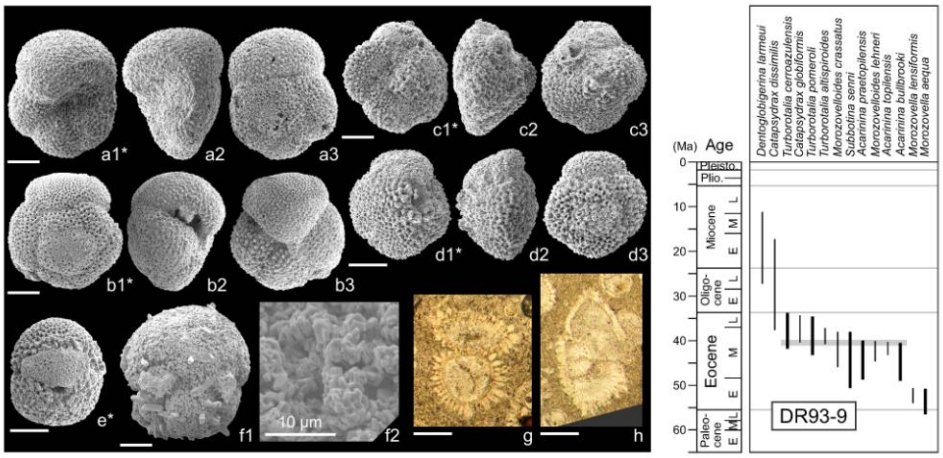

Ando et al. (2018MS)

Figure 4

100 % (167.5 × 80.0 mm)

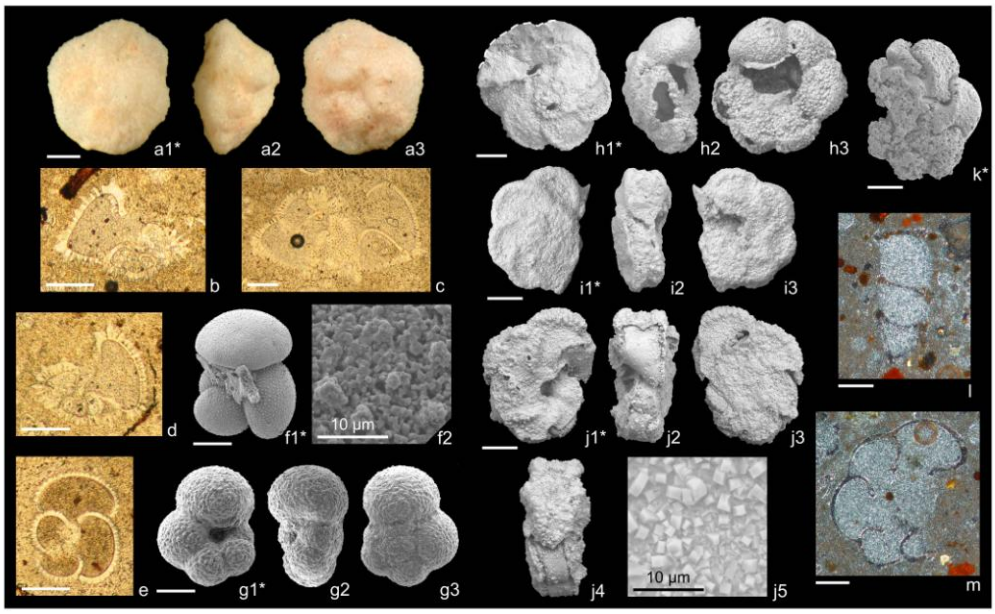

Ando et al. (2018MS)

Figure 5

100 % (177.0 × 108.0 mm)

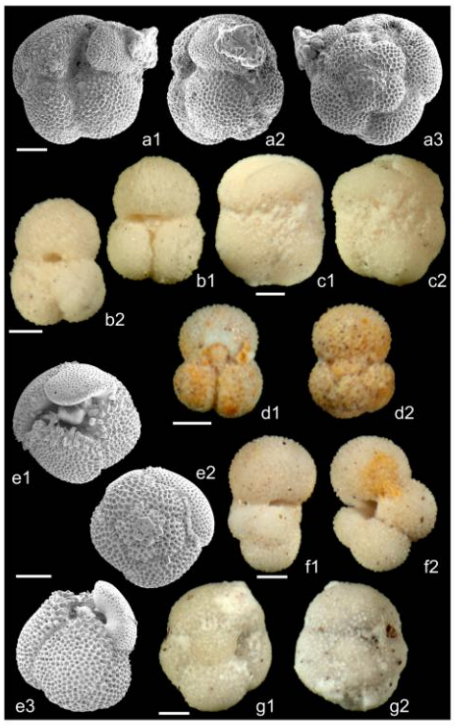

Ando et al. (2018MS)

Figure 6

100 % (80.0 × 128.0 mm)

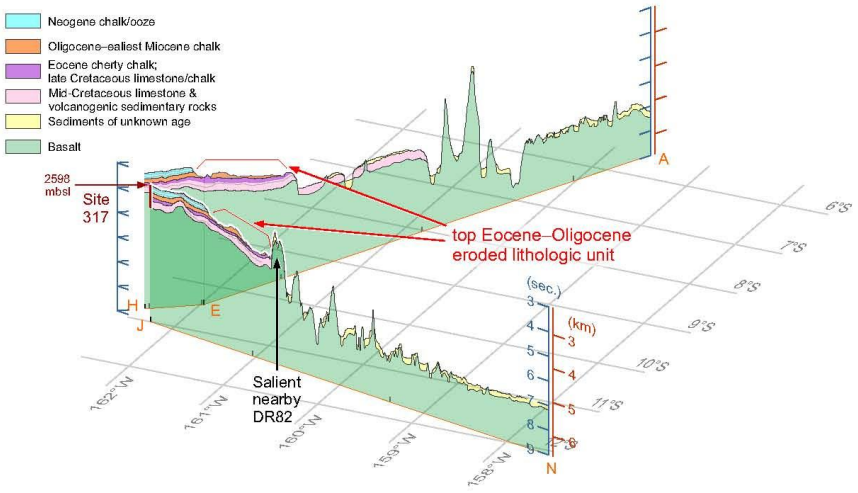

Ando et al. (2018MS)

Figure 7

100 % (151.9 × 86.1 mm)

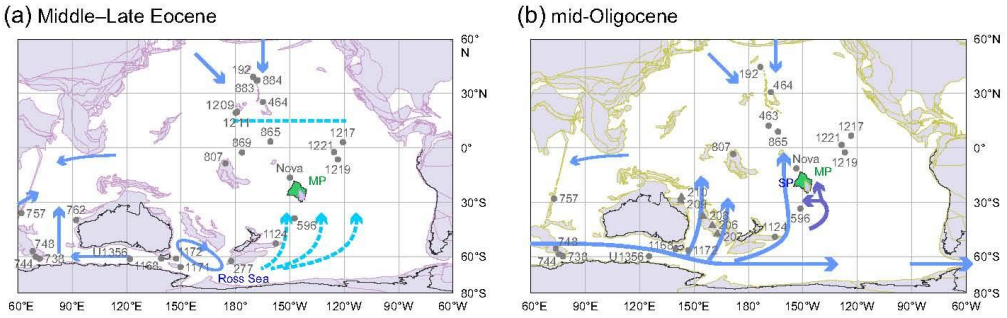

Ando et al. (2018MS)

Figure 8

100 % (178.4 × 54.7 mm)